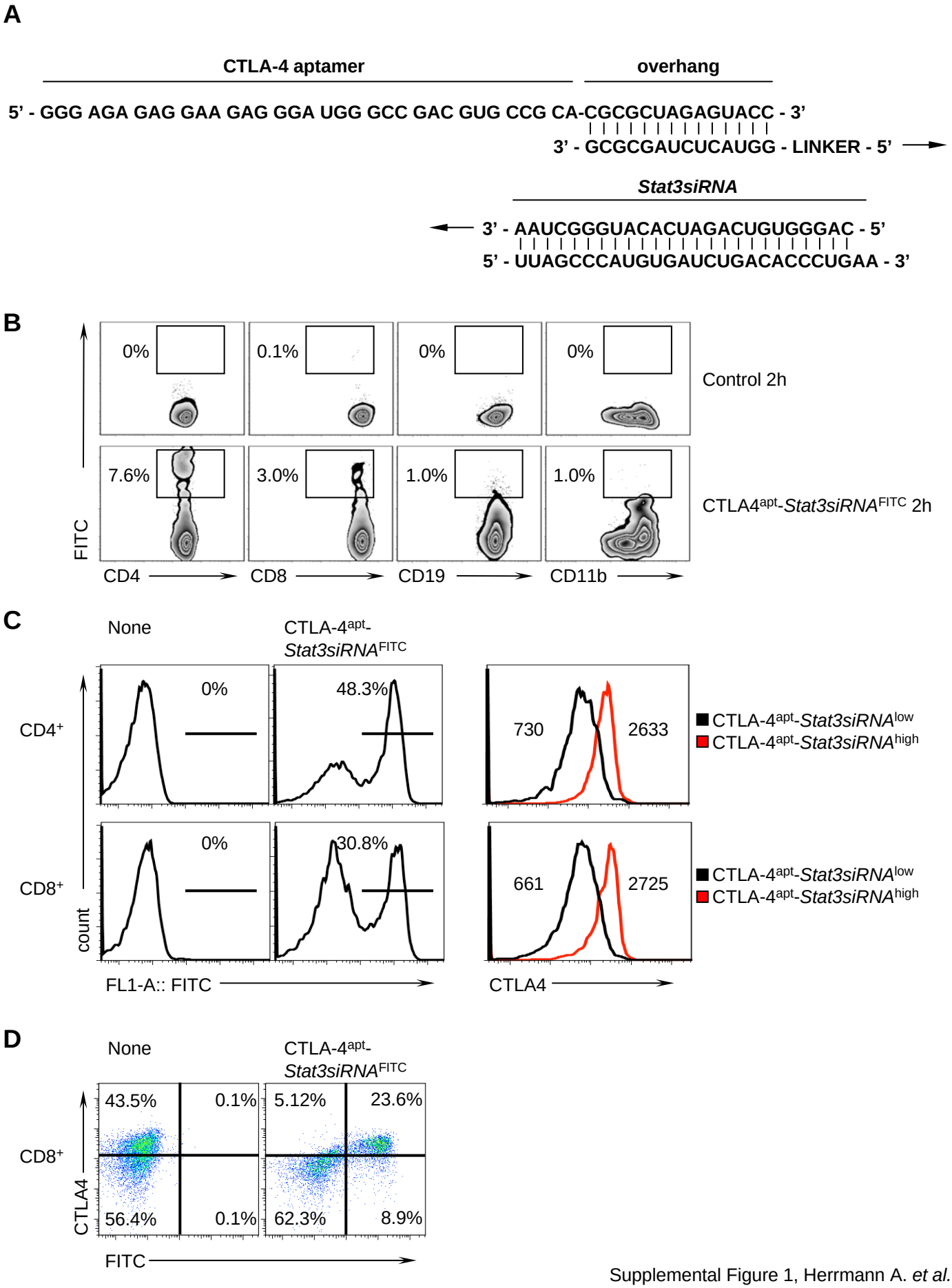


Supplemental Figure 1, Herrmann A. *et al.*

**E**

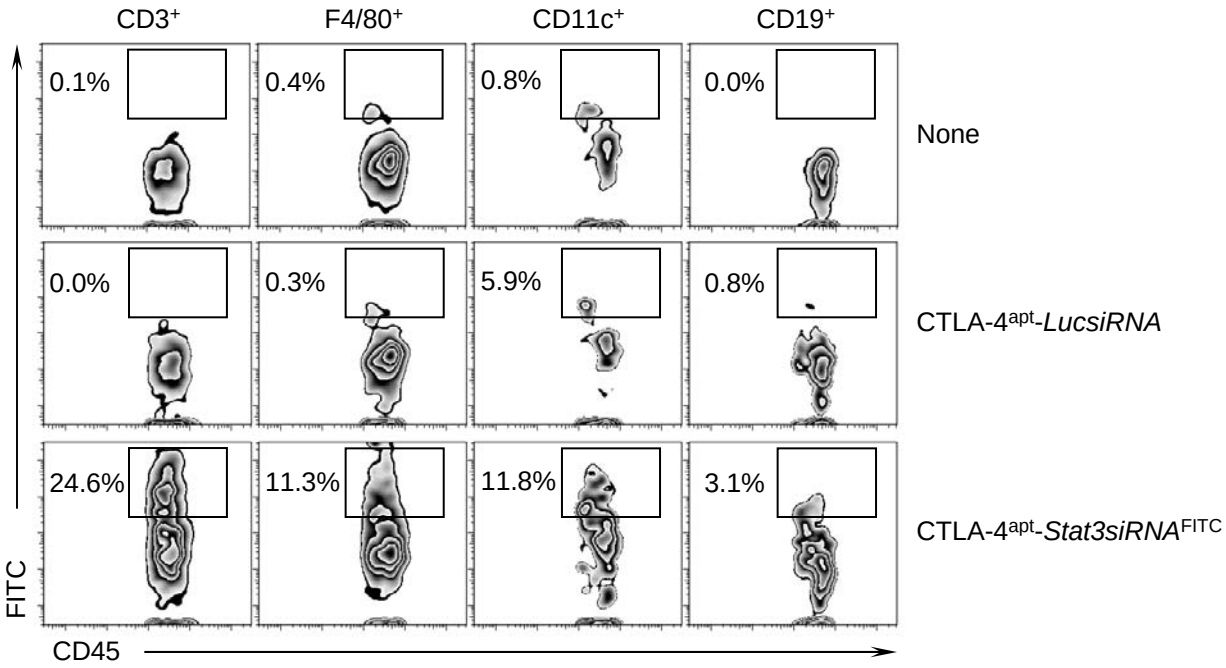


Supplemental Figure 1 cont'd, Herrmann A. *et al.*

**Supplemental Figure 1: CTLA4apt design and uptake in vitro and in vivo.**

(**A**) Scheme and sequences of the CTLA4aptamer with *Stat3siRNA* conjugate. (**B**) For in vitro uptake, total nucleated splenocytes from wild-type C57BL/6 mice were pre-stained with fluorophore-conjugated surface markers (CD4, CD8, CD19, and CD11b) and then 1 x $10^6$ cells were treated with control (untreated) or FITC-conjugated CTLA4$^{apt.}$*Stat3siRNA* (500 pmol/ml) for 2 hrs and analyzed by flow cytometry. Gating on CD4$^+$, CD8$^+$, CD19$^+$,CD11b$^+$ cells positive for CTLA-4$^{apt.}$*Stat3siRNA*-FITC. (**C**) Efficient cellular uptake of CTLA4$^{apt.}$*Stat3siRNA* is CTLA4 dependent. Splenocytes from wild-type C57BL/6 mice were pre-stained with fluorophore-conjugated surface markers (CD4, CD8), and then 1 x $10^6$ cells were treated with FITC-conjugated CTLA4$^{apt.}$*Stat3siRNA* (500 pmol/ml) for 2 h or left untreated, immediately followed by flow cytometry. Total uptake of CTLA4$^{apt.}$*Stat3siRNA* by CD4 and CD8 T cells are shown (left panels). Gating on CD4$^+$and CD8$^+$ cells positive for CTLA-4$^{apt.}$*Stat3siRNA*-FITC. Flow cytometric analysis shows total counts for CTLA-4 low expressing and CTLA-4 high expressing CTLA-4-aptamer conjugate uptake (right panels). (**D**) Flow cytometric analysis showing CTLA-4 expression by splenic CD8 cells facilitates CTLA4$^{apt.}$*Stat3siRNA* internalization. Cells were treated with FITC-conjugated CTLA4$^{apt.}$*Stat3siRNA* (500 pmol/ml) for 2 h or left untreated. Gating on CTLA-4$^+$ CD8 cells positive for CTLA-4$^{apt.}$*Stat3siRNA*-FITC. (**E**) For in vivo uptake, mice bearing established 8101 fibrosarcoma tumors were treated for 3 consecutive days with control (untreated), unconjugated CTLA4$^{apt.}$*LucsiRNA*, or FITC-conjugated CTLA4$^{apt.}$*Stat3siRNA*. Single-cell suspensions from tumors analyzed for FITC-positive cells by flow cytometry. Gating on CD3$^+$, F4/80$^+$, CD11c$^+$, and CD19$^+$ CD45$^+$ cells positive for CTLA-4$^{apt.}$*Stat3siRNA*-FITC.

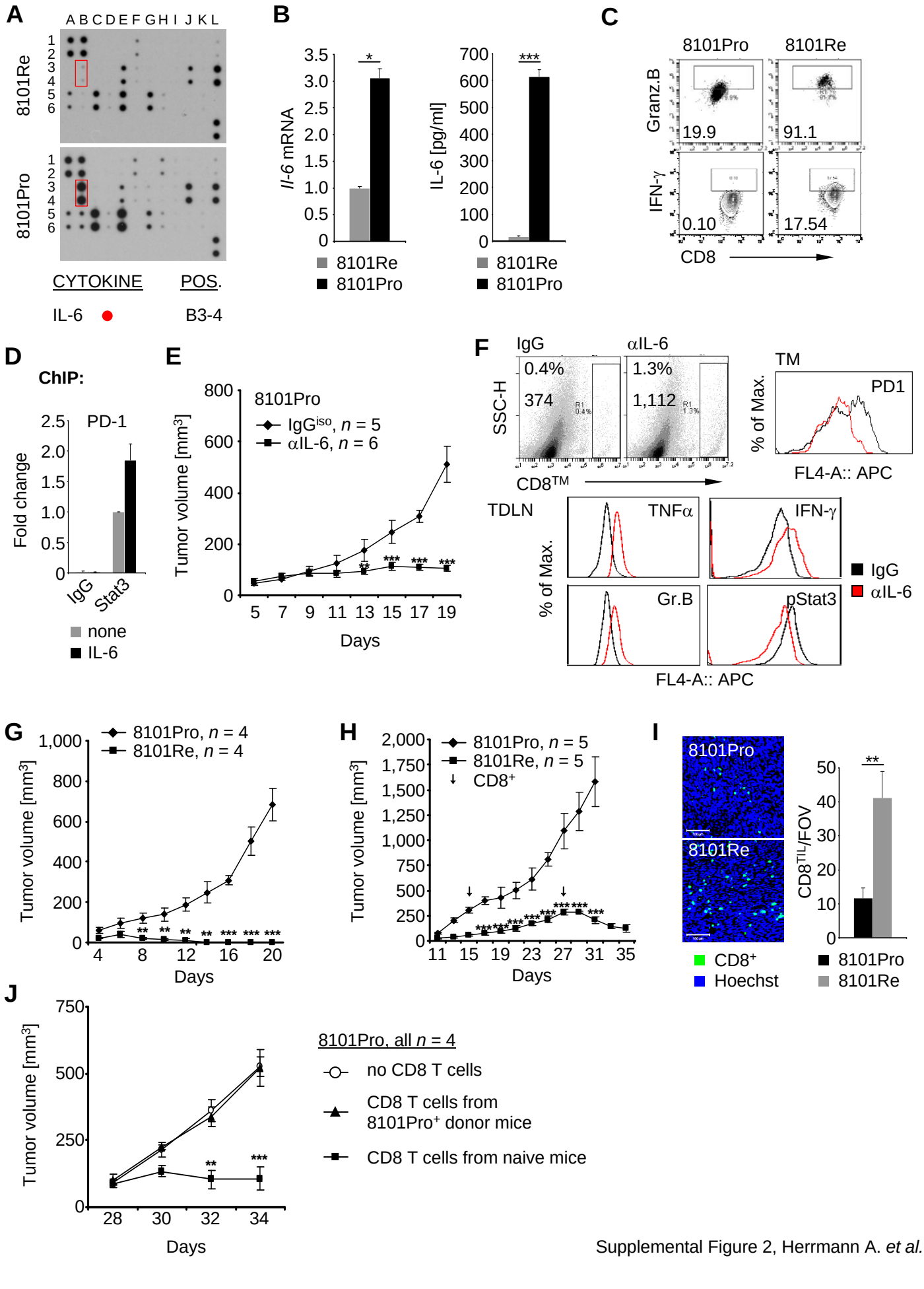


Supplemental Figure 2, Herrmann A. *et al.*

**Supplemental Figure 2: T cell tolerance in IL-6 overexpressing tumors.**

(**A**) Fibrosarcoma 8101Re and 8101Pro were analyzed for cytokine expression by cytokine arrays. (**B**) IL-6 expression by 8101Pro confirmed by RT-PCR (left) and ELISA (right). (**C**) Granzyme B and IFNγ expression by CD8 cells from 8101Re and 8101Pro tumors assessed by flow cytometry. Gating on $CD8^+$ cells positive for granzyme B and IFNγ, respectively. (**D**) IL-6 induces Stat3 binding to PD-1 promoter in CD8 T cells determined by ChIP assay. SD shown. (**E**) Depleting IL-6 with antibodies inhibits 8101Pro tumor growth. SD shown; t-test **) $P < 0.01$, ***) $P < 0.001$. (**F**) Effects of IL-6 depletion on tumor infiltrating CD8 cells (TILs) (upper left panels). Gating on $CD8^+$ TIL; PD-1 expression (upper right panel); TNFα, IFNγ, granzyme B and pStat3 expression in CTLs from TDLNs (lower panels). (**G**) 8101Re and 8101Pro tumor growth was acquired. (**H**) CD8 tolerance was determined monitoring tumor growth of 8101Re and 8101Pro in $Rag1^{-/-}$ mice receiving CD8 adoptive therapy (arrowhead). 8101Re regress upon adoptive transfer. 8101Pro growth relapsed. SD shown; t-test **) $P < 0.01$, ***) $P < 0.001$. (**I**) CD8 TILs visualized by confocal microscopy (left) and quantified (right). SD shown; t-test **) $P < 0.01$. (**J**) Tumor-induced T cell tolerance assessed by adoptive T cell transfer into B16 melanoma bearing mice comparing antitumor activity of CD8 cells isolated from tumor bearing donor mice with naïve CD8 cells. Untreated control included. SD shown; t-test **) $P < 0.01$, ***) $P < 0.001$.

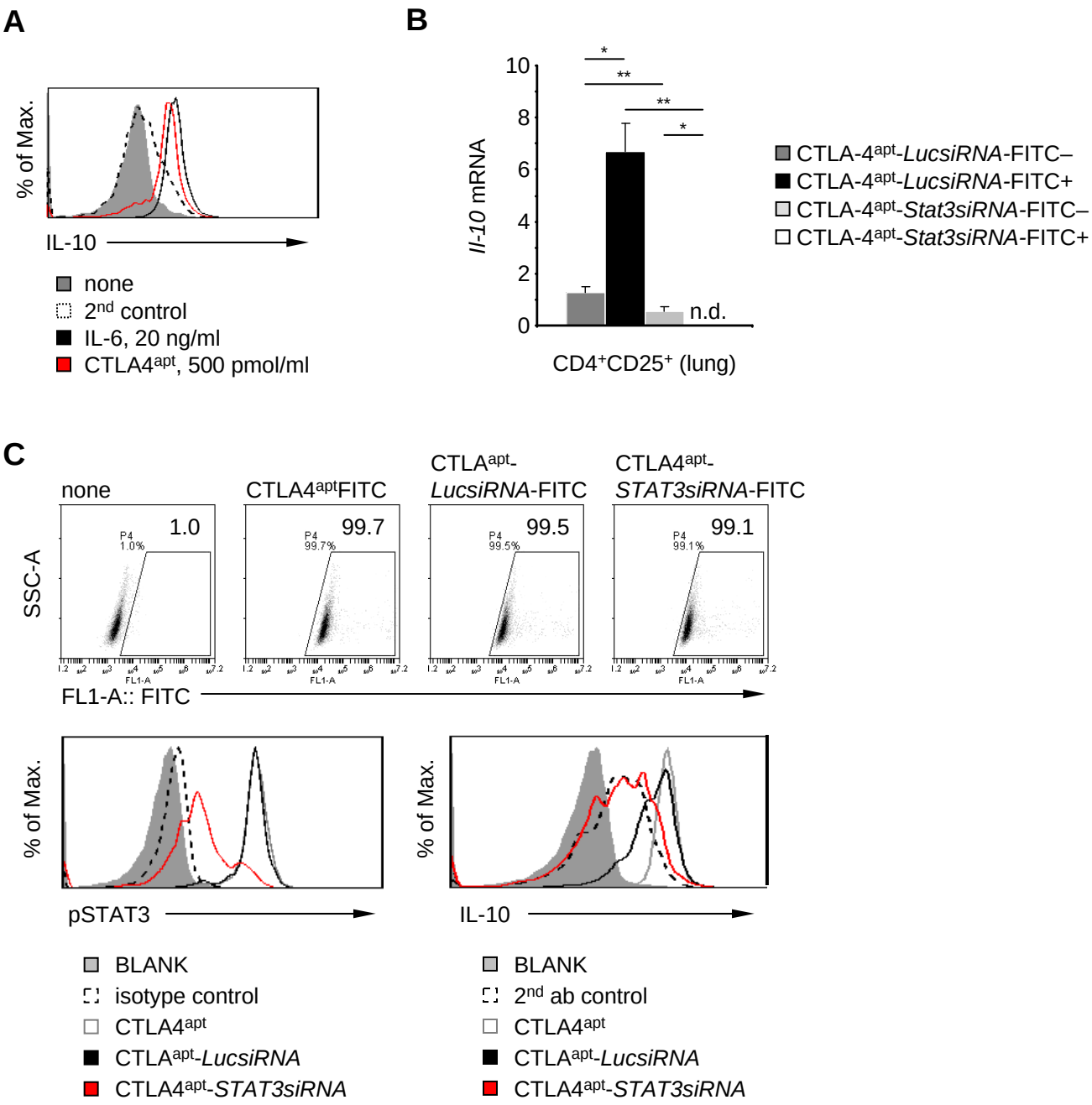


Supplemental Figure 3, Herrmann A. *et al.*

**Supplemental Figure 3: Effects of monomeric CTLA4-aptamer with or without siRNA linked.**

(**A**) Agonistic activity of monomeric CTLA4 aptamer was assessed by treating human Karpas299 T cell lymphoma cells with either 500 pmol/ml CTLA4-aptamer, 100 ng/ml IL-6 for 24 h or left untreated. IL-10 production was analyzed by flow cytometry. (**B**) IL-10 production is inhibited when CTLA4-apatmer is linked with Stat3siRNA. $CD4^{+}CD25^{+}$ $T_{Regs}$ were isolated by FACS sorting from lungs of mice with B16 melanoma metastasis/colonies after systemic treatments with fluorescently labeled $CTLA4^{apt.}$siRNA conjugates as indicated. Per single $CTLA4^{apt.}$siRNA-conjugate, $FITC^{+}$ and $FITC^{-}$ cells were obtained as indicated and analyzed for *Il-10* mRNA by RT-PCR. (**C**) Cellular uptake and Stat3 silencing in human Karpas299 lymphoma cells. Flow cytometry 500 pmol/ml of CTLA4-aptamer and $CTLA4^{apt.}$siRNA-conjugates for 2 h (upper panels). Gating on Karpas cells positive for aptamer-FITC conjugates. After 24 h of indicated treatments, pSTAT3 and IL-10 expression was analyzed by flow cytometry.

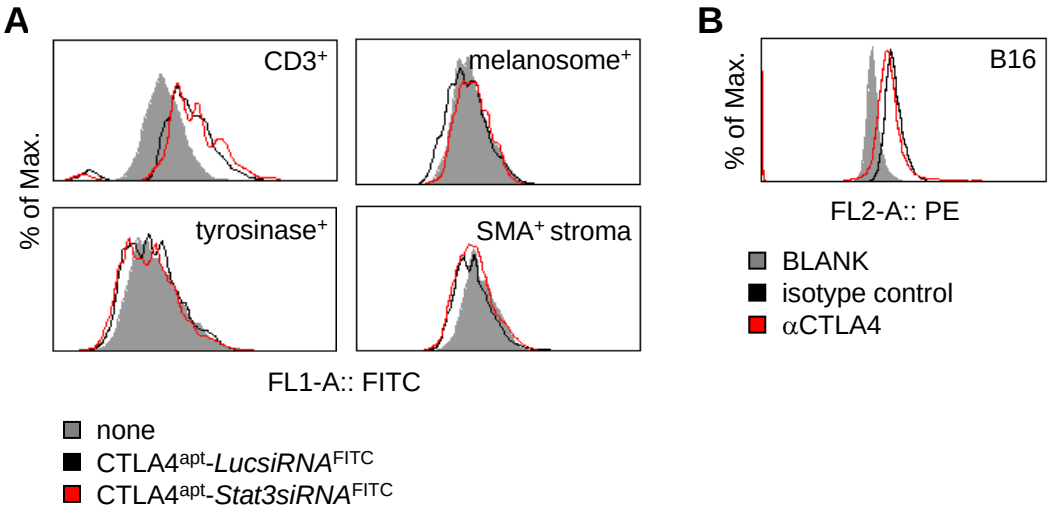


Supplemental Figure 4, Herrmann A. *et al.*

**Supplemental Figure 4: Selective CTLA4-aptamer conjugate uptake by the T cells.**

Mice injected with B16 melanoma cells to develop lung metastasis were treated with fluorescently labeled CTLA4-aptamer conjugates systemically. (**A**) Cellular uptake of aptamer-siRNA conjugates by $CD3^+$ T cells, melanoma cells (tyrosinase, melanosome) and smooth-muscle-$actin^+$ stromal cells was assessed by flow cytometry. (**B**) B16 melanoma cells do not express CTLA4 was shown by flow cytometry.

**A**

**CTLA-4 gene: full length**

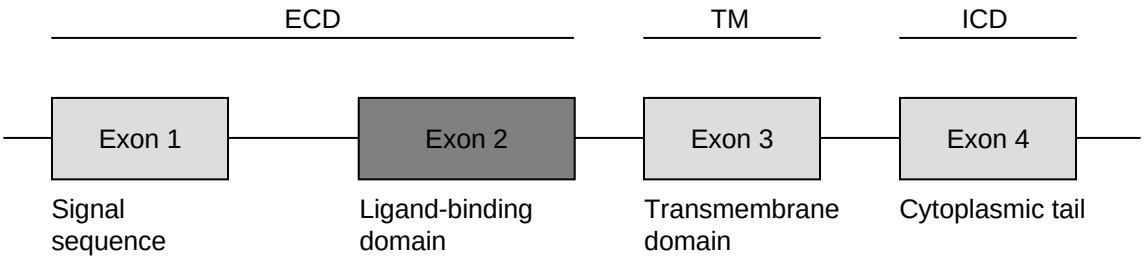


**B**

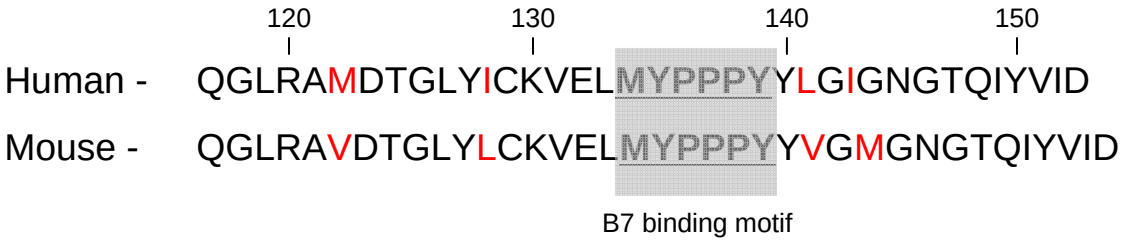


Supplemental Figure 5, Herrmann A. *et al.*

**Supplemental Figure 5: CTLA4 gene and its conservation.**

(**A**) Scheme of CTLA4 gene full length showing exons 1-2, which represent the extracellular domain (ECD), the transmembrane spanning region coded by exon 3, and the cytoplasmic tail coded by exon 4. (**B**) The amino acid sequence of the ligand binding region (B7 binding motif) of mouse and human CTLA-4 is highly conserved. (adapted from (29)).